

Backscattering anisotropy near 180° : an indication of particle size and shape

Wilhelmina R. Clavano¹
Cornell University
wrc22@cornell.edu

Emmanuel Boss
University of Maine
emmanuel.boss@maine.edu

Yogesh C. Agrawal
Sequoia Scientific, Inc.
yogi.agrawal@sequoiasci.com

Abstract

By modelling the single scattering of particles in the exact backward direction (180°) and 5° around, the field of view of an instrument measuring backscattering is simulated. Calculations of the scattering Mueller matrix M_{ij} using a development of the extended boundary condition method [1] are made for spheroidal particles with sizes (D in μ), shapes (defined by spheroidal aspect ratio $\frac{s}{t}$) and refractive indices similar to ($m = 1.05 + 0.01i$) marine particles found in the natural environment.

Results show that information about size and shape can be gathered from the intensity patterns of the backscattering for particles within the anomalous diffraction region (also known as the van de Hulst region). Comparison between the polarised scattering intensity patterns (I_{\parallel} and I_{\perp}) produced by these non-spheres and their volume-equivalent spheres provides insight into the information available from backscattering polarimetry on the effects of size and shape in light scattering by differently shaped particles.

“Effective” Mueller Matrices

- M_{11} and M_{44} remain anisotropic as size and shape change (Figs. 1 and 2).
- M_{11} , M_{22} , M_{44} , M_{12} , M_{23} , and M_{24} “contain” the general patterns.
- Except for M_{23} and M_{24} , these patterns are incorporated in I_{\parallel} and I_{\perp} .

All plots here are normalised; high values in red and low ones in blue.

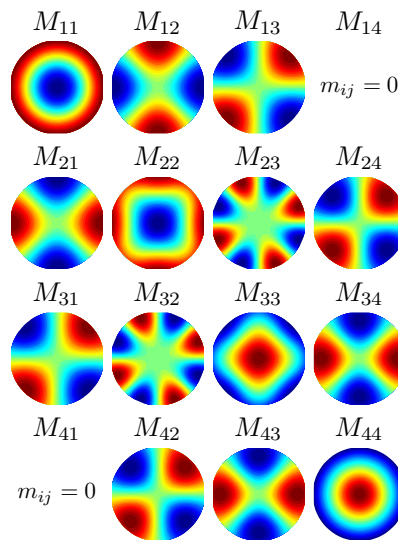


Figure 1: Spheres, $D = 5\mu$ and $\frac{s}{t} = 1$.

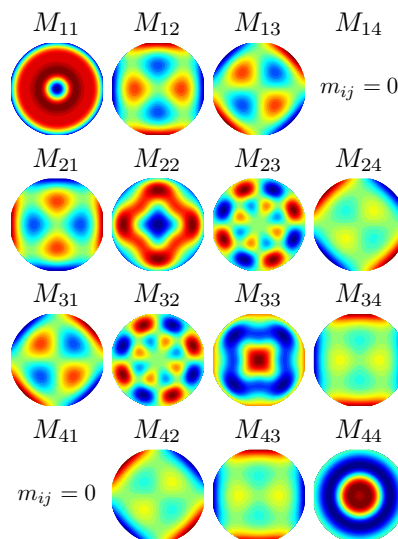


Figure 2: Spheroids, $D = 5\mu$ and $\frac{s}{t} = 0.46$.

Model Particles

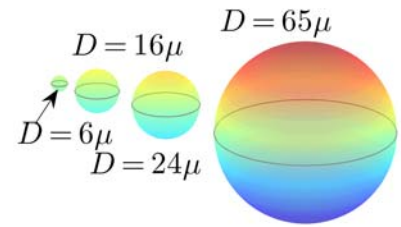


Figure 3: Increase in spherical size.

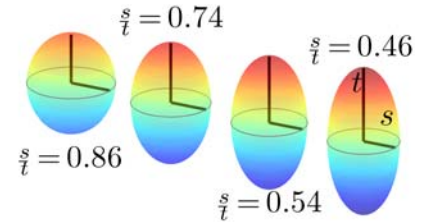


Figure 4: Increase in spheroidal shape.

Polarised Scattering Intensities

Fig. 5

- No depolarisation for **spheres** at 180° : $I_{\perp}(180^\circ) = 0$.
- **Number of minima and maxima** for I_{\parallel} and I_{\perp} increase with size (shown here only for spheres).
- Larger and larger particles will have patterns perceptibly similar to small ones as the undulations are drowned out.

Fig. 6

- The **width of the I_{\perp} peak** (or central peaks) increase with shape; more “cohesive” peaks with increasing refractive index.
- **Depolarisation for non-spheres** in the backward direction: $I_{\perp}(180^\circ) \neq 0$, although the pattern may be featureless.

¹Please see <http://www.people.cornell.edu/pages/wrc22/2006ASLO.html> for more information.

Appendix: Azimuthal Variation

- Start with the **scattering phase matrix**

$$\begin{bmatrix} F_{11} & F_{12} & 0 & 0 \\ F_{12} & F_{22} & 0 & 0 \\ 0 & 0 & F_{33} & F_{34} \\ 0 & 0 & -F_{34} & F_{44} \end{bmatrix}. \quad (1)$$

- An “**effective**” **Mueller matrix** is produced by taking into account the geometrical configuration of the imaging instrument (see [2], [3], [4])

$$\begin{bmatrix} M_{11} & M_{12} & M_{13} & 0 \\ M_{12} & M_{22} & M_{23} & M_{24} \\ M_{31} & M_{32} & M_{33} & M_{34} \\ 0 & M_{42} & M_{43} & M_{44} \end{bmatrix}. \quad (2)$$

- Apply **linearly polarised light** $[1; 1; 0; 0]$,
- a **Stokes vector** is produced $[I; Q; U; V]$.
- Derive the **intensity of parallel linear polarisation** (parallel to the incident direction, vertical in the plots)

$$I_{\parallel} = \frac{I+Q}{2} = \frac{1}{2}(M_{11} + 2M_{12} + M_{22}), \quad (3)$$

- and the **intensity of perpendicular linear polarisation**

$$I_{\perp} = \frac{I-Q}{2} = \frac{1}{2}(M_{11} - M_{22}). \quad (4)$$

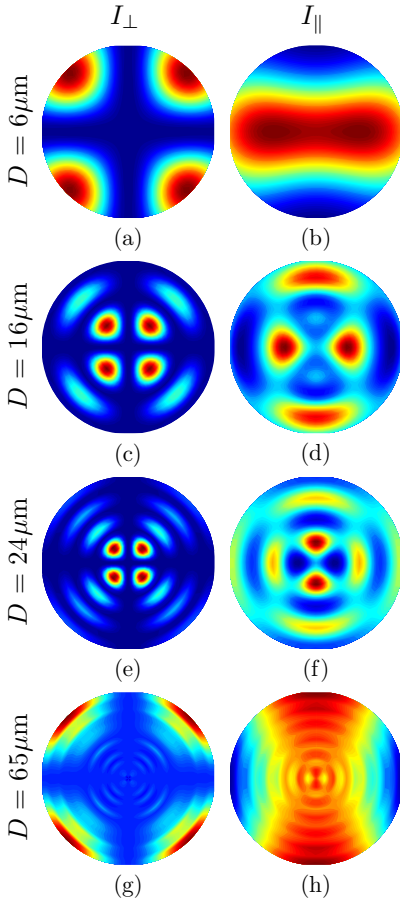


Figure 5: Size sensitivity.

Comment

Most backscattering comes from the smallest particles (in the anomalous diffraction region) of a natural marine population [7], so that backscattering polarimetry may be useful in detecting size and shape.

Acknowledgments. Amanda L. Whitmire of Oregon State University carried out the LISST measurements. Project support comes through ONR Ocean Optics and Biology.

References

- [1] Mishchenko and Travis 1998. *J. Quant. Spectrosc. Ra.* **60** (3): 309–324.
- [2] Pal and Carswell 1985. *Appl. Opt.* **24** (21): 3464–3471.
- [3] Bohren and Huffman 1998. *Absorption and Scattering of Light by Small Particles*. Wiley.
- [4] Yang, Wei, Kattawar, Hu, Winker, Hostetler and Baum 2003. *Appl. Opt.* **42** (21): 4389–4395.
- [5] Hu, Yang, Lin, Gibson and Hostetler 2003. *J. Quant. Spectrosc. Ra.* **79-80**: 757–764.
- [6] <http://www.sequoiasci.com>
- [7] Clavano, Boss and Karp-Boss 2006. *Oceanogr. Mar. Biol. Annual Review*. To be published July 2006.

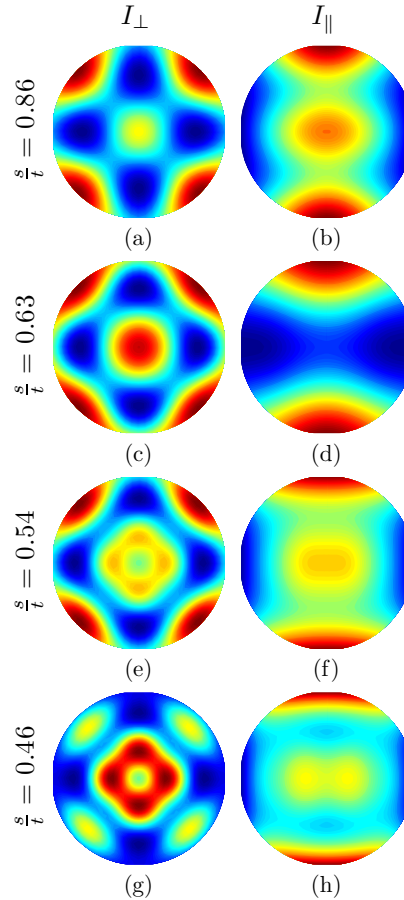


Figure 6: Shape sensitivity.

Size and Shape Effects

1. Interesting effects occur in the anomalous diffraction region: $\rho = \frac{2\pi D}{\lambda}(n-1)$, for $1 < \rho < 100$ where λ is the incident wavelength of light and n is the real part of the refractive index $m = n + ki$.
2. These theoretical calculations are compared with observations using a backscattering LISST developed by Sequoia Scientific, Inc. [6]: measurements of non-spheres (Fig. 7) show a spike in the backscatter direction while none for spheres (Fig. 8).
3. The area of the backscattering peak is expected to increase with shape.
4. How the peaks behave for larger particles and polydispersions is the objective of current comparisons.

LISST Measurements

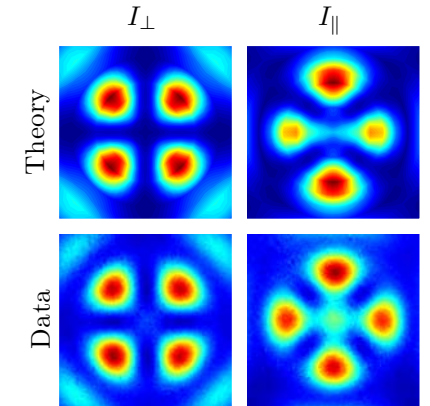


Figure 7: Comparison with data for spheres from the LISST shows qualitative “calibration”.

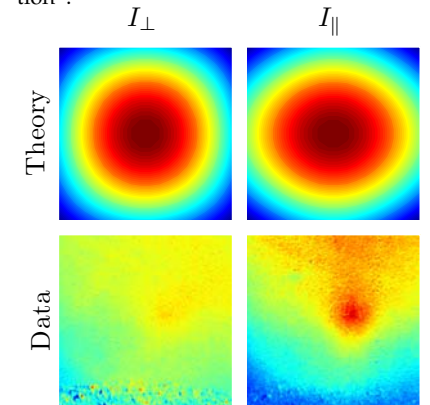


Figure 8: Particles 4 times smaller used for theoretical results; preliminary measurements of dust representing non-spheres.